Intrarenal cells, not bone marrow–derived cells, are the major source for regeneration in postischemic kidney

Fangming Lin,[1] Ashley Moran,[1] and Peter Igarashi[2]

[1]Department of Pediatrics and [2]Department of Internal Medicine and Division of Basic Sciences, University of Texas Southwestern Medical Center at Dallas, Dallas, Texas, USA.

Ischemic injury to the kidney produces acute tubular necrosis and apoptosis followed by tubular regeneration and recovery of renal function. Although mitotic cells are present in the tubules of postischemic kidneys, the origins of the proliferating cells are not known. Bone marrow cells (BMCs) can differentiate across lineages to repair injured organs, including the kidney. However, the relative contribution of intrarenal cells and extrarenal cells to kidney regeneration is not clear. We produced transgenic mice that expressed enhanced GFP (EGFP) specifically and permanently in mature renal tubular epithelial cells. Following ischemia/reperfusion injury (IRI), EGFP-positive cells showed incorporation of BrdU and expression of vimentin, which provides direct evidence that the cells composing regenerating tubules are derived from renal tubular epithelial cells. In BMC-transplanted mice, 89% of proliferating epithelial cells originated from host cells, and 11% originated from donor BMCs. Twenty-eight days after IRI, the kidneys contained 8% donor-derived cells, of which 8.4% were epithelial cells, 10.6% were glomerular cells, and 81% were interstitial cells. No renal functional improvement was observed in mice that were transplanted with exogenous BMCs. These results show that intrarenal cells are the main source of renal repair, and a single injection of BMCs does not make a significant contribution to renal functional or structural recovery.

Introduction

Ischemia/reperfusion injury (IRI) of the kidney causes necrosis and apoptosis of renal tubular epithelial cells (1, 2). Dead cells detach from the tubular basement membrane, leaving denuded basement membrane. Over time, the injured tubules regenerate through cell proliferation, as reflected by the expression of proliferating cell nuclear antigen (PCNA) (3). Tubular regeneration restores normal tubular architecture and renal function. However the source of the proliferating cells that repopulate the injured nephron is not clear. Tissue regeneration may result from proliferation and differentiation of resident stem/progenitor cells, proliferation of surviving dedifferentiated cells, or "transdifferentiation" of cells that originate from outside the injured organ (1, 4–11). In this study we tested whether kidney regeneration fits into this general paradigm.

Recently, Oliver et al. discovered that the renal papilla is a niche for adult kidney stem cells. These slow-cycling cells can proliferate and may participate in renal regeneration after ischemic injury (12). In addition to increased proliferative activity, regenerating tubules show decreased cellular differentiation following IRI. Several genes that are expressed during embryonic development and are downregulated in the mature kidney are reexpressed during recovery from renal injury (13). One example is the transcription factor paired box gene 2 (Pax2), which is transiently expressed
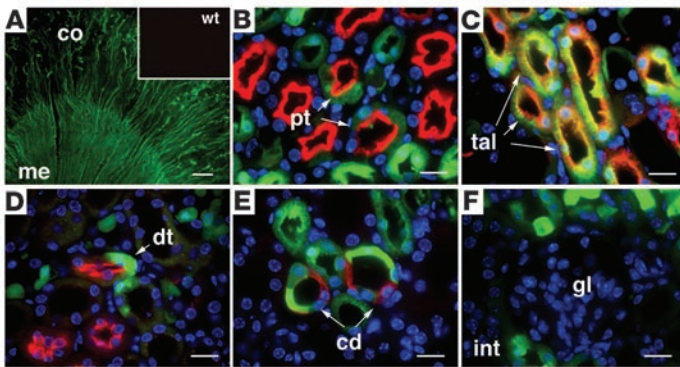
in developing nephrons during early nephrogenesis and is reexpressed in regenerating proximal tubules (14). The intermediate filament vimentin is expressed in the metanephric mesenchymal cells that are the progenitors of the epithelial cells of the nephron. Vimentin is normally not significantly expressed in well-differentiated renal tubular epithelial cells but is reexpressed in injured tubular cells (3). Based on these observations, it has been postulated that the cells that regenerate injured tubules are derived from surviving tubular epithelial cells that dedifferentiate and reenter the cell cycle (3, 15). However, no studies have directly proven that this is the case.

Another potential source of regenerating tubular cells is cross-lineage differentiation of cells that are of extrarenal origin. There is increasing evidence that circulating stem cells can enter the kidney and differentiate into renal cells after various injuries. We and others have shown that bone marrow cells (BMCs) can differentiate into tubular epithelial cells, glomerular endothelial cells, podocytes, mesangial cells, and renal interstitial cells (16–22). After transplanting hematopoietic stem cells isolated from male Rosa26 mice, we detected cells expressing β-gal in the renal tubules in female wild-type mice that had renal IRI. The male-specific sex determining region of chromosome Y (Sry) gene and cells carrying a Y chromosome were also detected in the kidney (16). In male patients who received kidney transplants from female donors, Y chromosome–containing cells that expressed renal tubular cell markers were observed in kidneys that had sustained injury due to a variety of causes (18, 19). Morigi et al. showed that bone marrow mesenchymal stem cells could differentiate into renal tubular epithelial cells and improve renal function (23). However, the relative contribution of extrarenal cells and intrarenal cells to kidney regeneration has not been evaluated. In addition, the formation of different types of renal cells from BMCs has not been examined

Figure 1
Genetic marking of renal tubular epithelial cells with EGFP in *cre^ksp;Z/EG* mice. (**A**) Expression of native EGFP fluorescence in frozen section of the kidney. co, cortex; me, medulla. The inset shows that green fluorescence is absent in the kidney of a wild-type littermate photographed under the identical exposure conditions. (**B–E**) Paraffin sections of the kidney stained with anti-EGFP antibody (green) and antibodies or lectins that stain specific nephron segments (red) showing the presence of EGFP in LTA-positive proximal tubules (pt, **B**); THP-positive thick ascending limbs (tal, **C**); TSC-positive distal tubules (dt, **D**); and DBA-positive collecting ducts (cd, **E**). (**F**) Absence of EGFP in the glomeruli (gl) and interstitium (int). The nuclei were counterstained with DAPI, and images were merged in (**B–F**) Scale bars: 400 μm in **A** and 20 μm in **B–F**.

systematically in a single study. We sought to address the relative importance of intrinsic renal cells and BMCs in kidney regeneration, as well as the plasticity of BMCs in forming kidney cells.

Results

Lineage marking of renal tubular epithelial cells with enhanced GFP. To measure the contribution of intrinsic renal cells to tubular regeneration, we performed lineage analysis using cre/loxP recombination. The *Z/EG* double reporter mouse strain carries a ubiquitous promoter linked to a *lacZ* gene that is flanked by 2 *loxP* sites and an enhanced GFP (EGFP) reporter gene that resides further downstream (24). In the absence of cre recombinase, *lacZ* is expressed in most tissues, including kidney cells. In the presence of cre recombinase, recombination between the *loxP* sites deletes the *lacZ* sequence and activates the *EGFP* reporter gene. Since the activation of the reporter gene is irreversible and heritable, EGFP will be expressed in all progeny cells irrespective of the continued presence of cre recombinase. Therefore, the fate of the cre-expressing cells can be easily traced.
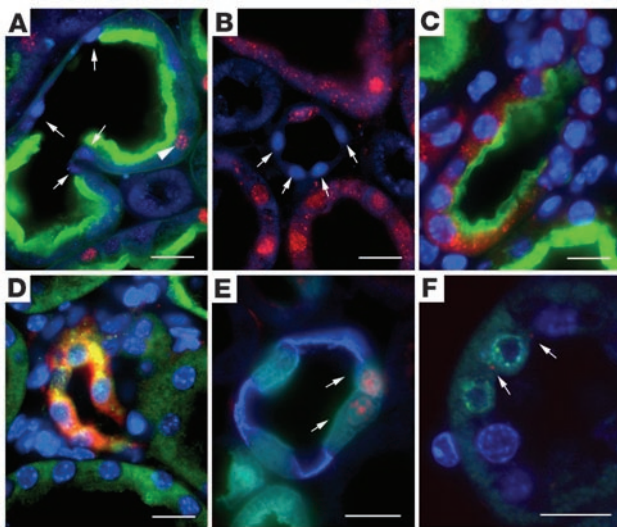
Figure 2
Tubular injury and cell proliferation in EGFP-expressing tubular epithelial cells. PAS staining and immunostaining were performed in the kidney sections of *cre^ksp;Z/EG* mice with renal IRI. (**A**) PAS staining of the kidney at 2 days after IRI. Tubular injury is shown by the loss of brush border membrane, cell detachment from the basement membrane, and nuclear condensation in some cells (arrows). (**B**) Expression of PCNA in tubular cells (red, arrows). (**C**) Low-power image of BrdU incorporation in renal tubules. Some BrdU-containing cells (red, arrows) colocalized with EGFP-expressing cells (green). The arrowhead indicates BrdU incorporation in an EGFP-negative cell. (**D**) BrdU incorporation (red, arrow) in the epithelial cells expressing EGFP (green). The nuclei were counterstained with DAPI, and images were merged (**B–D**). Scale bars: 20 μm.

To label renal tubular epithelial cells, we crossed *Z/EG* mice with *cre^ksp* transgenic mice that express cre recombinase under the control of the kidney-specific Ksp-cadherin promoter (ksp). Previous studies have shown that *cre^ksp* mice express cre exclusively in tubular epithelial cells in the kidney (25). Cre is expressed in all segments of the nephron, including proximal tubules, loops of Henle, distal tubules, and collecting ducts. There is no expression in blood vessels, glomerular cells, or interstitial cells. During embryonic development, cre is only expressed in maturing renal tubules and collecting ducts. There is no expression in early nephric structures, including mesenchymal condensates, renal vesicles, or comma- and S-shaped bodies. Therefore, crosses between *cre^ksp* mice and *Z/EG* mice should generate *cre^ksp;Z/EG* offspring in which mature renal tubular epithelial cells and their progeny are permanently labeled with EGFP. Continuous expression of EGFP is independent of the *ksp* promoter. Tracking EGFP-expressing cells in regenerating kidneys thus permits studies of tubular epithelial cell fate during renal repair.

Figure 1 shows the kidneys of *cre^ksp;Z/EG* mice analyzed at 6 weeks of age. Native EGFP fluorescence was detected in tubules in the renal cortex and medulla (Figure 1A), whereas under identical exposure conditions, green fluorescence was absent in kidneys of wild-type littermates (Figure 1A, inset). To identify the nephron segments in which EGFP was expressed, we stained paraffin sections of the kidneys with an anti-EGFP antibody and then with renal tubular markers. EGFP was expressed in proximal tubules that were labeled with *Lotus tetragonolobus* agglutinin (LTA), thick ascending limbs that expressed Tamm-Horsfall protein (THP), distal tubules that expressed the thiazide-sensitive Na-Cl cotransporter (TSC), and collecting ducts that were labeled with *Dolichos biflorus* agglutinin (DBA) (Figure 1, B–E). Especially in the proximal and distal tubules, EGFP was expressed in some cells but not in others, which indicated that the expression was mosaic. The mosaic expression pattern of EGFP in *cre^ksp;Z/EG* mice was due to inefficient cre/loxP
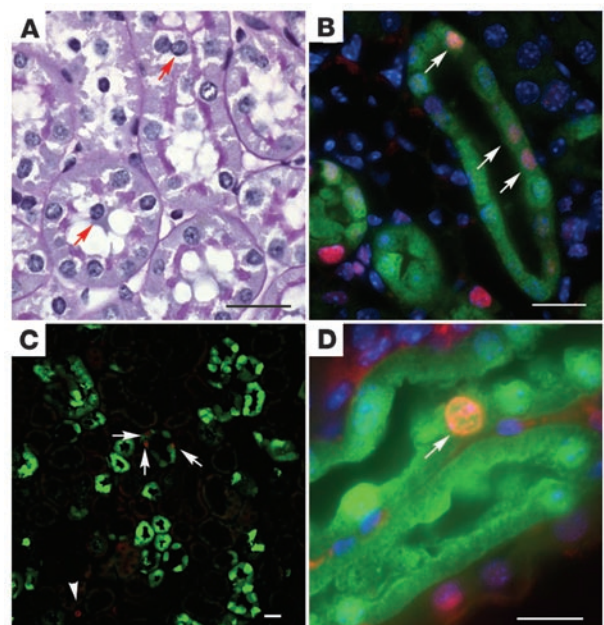
Figure 3
Dedifferentiation of epithelial cells during repair of renal tubules. Immunostaining was performed in kidney sections of $cre^{ksp};Z/EG$ mice with renal IRI. (**A**) Expression of Pax2 (blue, arrows) in LTA-positive (green) proximal tubules. Note the nuclear localization of Pax2 in the injured area lacking brush border staining of LTA. The same tubule also contains cells that incorporated BrdU (red, arrowhead). (**B**) Down-regulation of p21 (red) in cells expressing Pax2 (blue, arrows). (**C**) Expression of vimentin (red) in LTA-positive (green) proximal tubule. (**D**) Expression of vimentin (red) in epithelial cells expressing EGFP (green). Cells coexpressing vimentin and EGFP appear yellow. (**E**) An EGFP-expressing cell (green, arrow) shows incorporation of BrdU (red) and basolateral expression of AQP3 (blue). (**F**) Cells that incorporated BrdU (green) established intercellular junction and expressed ZO-1 (red, arrows). The nuclei were counterstained with DAPI (**C**, **D**, and **F**), and images were merged. Scale bar: 20 μm.

recombination and heterocellular activity of the Z/EG promoter. Antibody staining showed that 45% of the renal tubules in cre^{ksp} mice expressed cre protein. In Z/EG mice, 53% of tubular cells were X-gal positive. In the bitransgenic offspring of cre^{ksp} and Z/EG mice, we detected EGFP in 34% of tubular cells. Glomerular and interstitial cells showed no expression of EGFP (Figure 1F), which is consistent with the tubular epithelial cell–specific activity of the Ksp-cadherin promoter (25, 26).

Tubular regeneration from intrarenal cells. Female $cre^{ksp};Z/EG$ mice (6–8 weeks old) were subjected to 45 minutes of unilateral IRI of the left kidney, as described previously (13). To simultaneously measure the incorporation of exogenous bone marrow stem cells, the mice were injected with BMCs isolated from male C57BL/6 mice. Age-matched, sham-operated mice were given BMC injection as a control. The left kidneys showed extensive tubular necrosis and apoptosis, with loss of brush border membrane, cell detachment from the basement membrane, and nuclear condensation in some cells (Figure 2A). Cell death was followed by cell proliferation, as evidenced by PCNA expression in the outer stripe of the outer medulla at 2 days after IRI (Figure 2B). This region of the kidney contains the S3 segments of proximal tubules that are particularly susceptible to ischemic injury. PCNA expression in postischemic kidney was time dependent. At 1 day after IRI, 9.4% ± 2.0% of the tubular cells expressed PCNA, and the expression was higher at 2 days (34% ± 5.1%; $n = 4$). In

contrast, PCNA expression in age-matched control kidneys was 0.68% ± 0.07% at 2 days following sham operation ($n = 4$). At 7 days after IRI, PCNA expression declined to 16% ± 2.5%, and at 28 days, only 0.2% ± 0.04% of the cells expressed PCNA, which was not significantly different from the level of 0.07% observed in age-matched control kidneys.

We measured BrdU incorporation to evaluate cell regeneration (10). Mice were injected with BrdU for 14 days following ischemic injury, and then the kidneys were removed, sectioned, and stained with an anti-BrdU antibody. Figure 2C is a low-power image of the postischemic kidney showing BrdU incorporation in tubular cells, some of which expressed EGFP. At 28 days, 7.6% ± 0.3% of tubular cells incorporated BrdU when an average of 1,100 nuclei were counted on 2 adjacent kidney sections ($n = 3$). In contrast, only 0.4% ± 0.13% tubular cells incorporated BrdU in sham-operated mouse kidneys ($n = 4$). Most of the BrdU-positive cells were located in the outer stripe of the outer medulla and stained positive with LTA, which indicates that they represented S3 segments of proximal tubules. BrdU-positive cells were also detected in THP-expressing thick ascending limbs and aquaporin-2–expressing collecting ducts (data not shown). These results indicated robust tubular regeneration after injury. Costaining of the ischemic kidney with antibodies to BrdU and EGFP showed that BrdU was incorporated into the DNA of EGFP-positive cells (Figure 2D). These results provide direct evidence for tubular regeneration from EGFP-expressing tubular cells.

BrdU incorporation was also observed in the contralateral nonischemic kidney (data not shown). However, we did not detect BrdU in EGFP-positive cells in the uninjured kidney. To evaluate the degree of cell regeneration from EGFP-expressing cells, we measured the number of EGFP-expressing cells in the proximal tubules, the sites where more injury and regeneration occurs. As indicated by the mosaic pattern of EGFP expression in $cre^{ksp};Z/EG$ mice, not all the proximal tubular cells expressed EGFP. Because the baseline level of EGFP expression in the proximal tubules was low, changes were quantifiable, whereas in the distal nephron, the baseline expression was too high to allow detection of a change in the percentage of labeled cells. In the injured kidney, 54% ± 4.9% of proximal tubular cells were EGFP positive, whereas 34% ± 7.8% of proximal tubular cells in the uninjured kidney were EGFP positive. The difference in the percentage of EGFP-expressing cells between injured and uninjured cells was statistically significant ($n = 4$; $P < 0.05$). Taken together, these results suggest that epithelial cells are the main precursors for tubular repair, which accounts for the increased number of EGFP-positive cells in the proximal tubule in the kidneys that had recovered from injury.

Dedifferentiation of mature epithelial cells as the mechanism of renal repair. The expression of 2 dedifferentiation markers, Pax2 and vimentin, was examined in the regenerating kidneys (3, 14). At 3 days after injury, cells in some areas of the proximal tubules lacked a brush border, as indicated by the absence of LTA staining. The cells in these regions expressed Pax2 (Figure 3A). In the proximal tubules where Pax2 was reexpressed, 37% ± 0.2% of the cells incorporated BrdU ($n = 3$). No proximal tubular expression of Pax2 was observed in sham-operated kidneys or the contralateral nonischemic kidney. The expression of the cyclin-dependent kinase inhibitor p21 was downregulated in the tubules that expressed Pax2 (Figure 3B). Vimentin, a marker for dedifferentiated tubular cells, was detected in the proximal tubules (Figure 3C). Importantly, vimentin was expressed in EGFP-positive cells (Figure 3D), which indicated
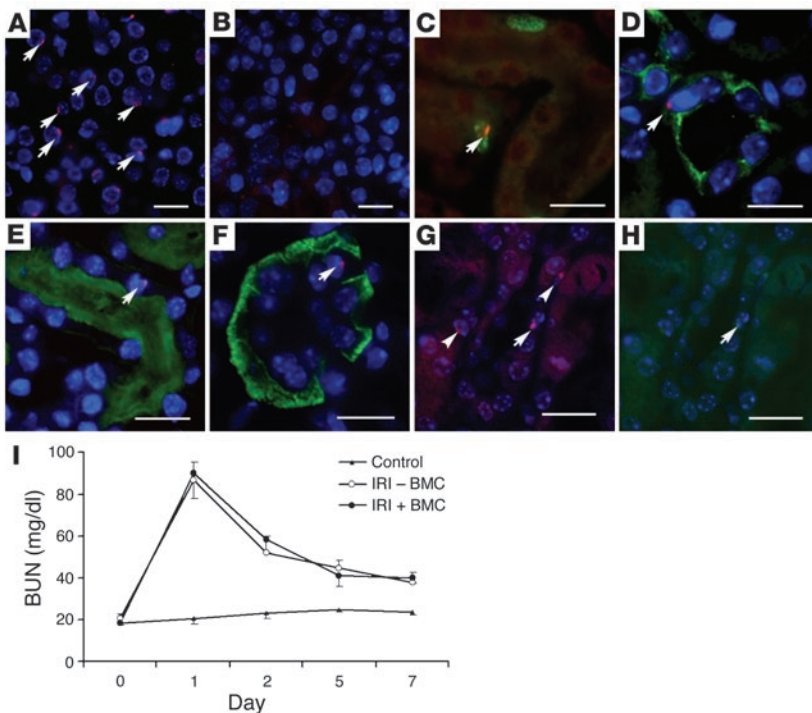
Figure 4

Effects of BMCs on tubular regeneration (**A–H**) and renal function (**I**). (**A**) Abundant Y chromosome signals located at the periphery of the nuclei in the kidneys of male mice (red, arrows), consistent with the typical nuclear localization of the Y chromosome. The sensitivity of FISH analysis was 64% (*n* = 5). (**B**) Kidney of a female mouse without male BMC transplant shows complete absence of Y chromosome signal. (**C**) A tubular cell that incorporated BrdU (green) shows the presence of Y chromosome (red, arrow). (**D–F**) Y chromosome FISH (red) was followed by immunostaining of tubular epithelial cell markers (green). (**D**) The arrow indicates a Y⁺ cytokeratin⁺ tubular epithelial cell. (**E**) The arrow indicates a Y⁺ LTA⁺ proximal tubular cell. (**F**) The arrow indicates a Y⁺ AQP3⁺ collecting duct cell. Note the basolateral staining of the AQP3, which defines the intratubular localization of the Y⁺ cells. (**G**) Y chromosome–containing tubular cell (arrows) in the kidney of a wild-type female mouse injected with BMCs from a male *cre^ksp;Z/EG* donor. Arrowheads indicate interstitial cells. (**H**) The same cell shown in **G** is negative for EGFP by immunostaining (arrow). The nuclei were counterstained with DAPI (**A**, **B**, and **D–H**), and images were merged. Scale bars: 20 μm. (**I**) BUN levels in mice with sham operation that did not receive BMC injection (Control; filled triangles), mice with renal IRI that did not receive BMC injection (IRI – BMC; open circles), and mice with renal IRI that received BMC injection (IRI + BMC; filled circles). No statistically significant difference was observed in mice with or without BMC injection. *n* = 5–13 at each time point; total 84 mice.

genic female mice that received BMCs from 6- to 8-week-old wild-type male donors. To distinguish male cells from female cells, we performed Y chromosome FISH and identified proliferating cells by anti-BrdU staining. Kidneys were harvested at 28 days after injury, a time point at which kidney regeneration is completed, and 4-μm-thick sections were hybridized with a Y chromosome painting probe. We measured the sensitivity and specificity of Y chromosome FISH by analyzing kidneys from male and female mice that did not receive BMC transplants. Abundant Y chromosome signals were detected at the periphery of the nuclei in the cells of kidneys of male mice (Figure 4A). The sensitivity of FISH was calculated as 64% (*n* = 5). In contrast, in the female kidney, there was a complete absence of Y chromosome signals (Figure 4B; *n* = 5), which corresponded to a specificity of 100%. BrdU-positive cells, Y chromosome–positive cells, and total tubular cells were counted in 10 randomly selected fields in the outer stripe of outer medulla (*n* = 4). The results are summarized in Table 1. The percentage of Y chromosome–positive cells was corrected for the 64% sensitivity of Y chromosome FISH analysis. Among all BrdU-positive cells in the tubules, 89% did not contain a Y chromosome, which indicated that they originated from host cells. The remaining 11% of the tubular cells contained a Y chromosome, which indicated that they originated from injected BMCs. Therefore, intrinsic renal cells are the major source for renal tubular regeneration.

BMCs can become renal tubular epithelial cells. We have previously shown that transplantation of sorted hematopoietic stem cells isolated from male Rosa26 mice into nontransgenic female recipients after renal IRI resulted in the appearance of β-gal–positive cells in the proximal tubules (16). In addition, PCR of the male-specific *Sry* gene and Y chromosome FISH showed the presence of male-derived cells in the female kidney. To more clearly define the donor-derived cells in the kidneys, we performed Y chromosome FISH followed by immunohistochemistry (27). Twenty-eight days after injury, incorporation of BrdU was detected in Y chromosome–positive cells in the renal tubules, which indicated proliferation of BMC-derived cells (Figure 4C). No CD45-positive cells were detected in the tubules, which indicated the absence of infiltrating hematopoietic cells (tubulitis). To confirm the formation of renal tubular epithelial cells from BMCs, we performed Y chromosome FISH analysis followed by immunostaining with the epithelial cell marker cytokeratin. Y chromosome was detected in cells expressing cytokeratin (Figure 4D). Renal proximal tubules sustain the most injury and are most active in regeneration in mouse models of IRI (3, 28). Staining with the proximal tubule–specific lectin LTA showed the presence of Y chromosome in proximal tubular cells (Figure 4E). BMC-derived cells were also observed in the collecting duct, a segment that is thought to be relatively resistant to IRI (3). The Y chromosome–positive collecting duct cells expressed

that the dedifferentiated cells originated from preexisting mature tubular epithelial cells. In the contralateral kidney, no expression of vimentin was detected in any tubules. At 28 days after IRI, no expression of vimentin was detected in any tubules, and Pax2 was no longer detected in the proximal tubules. These results indicate that regenerated tubules had become mature epithelial cells.

EGFP-expressing cells that incorporated BrdU reestablished cell polarity, as indicated by the presence of AQP3 on the basal cell membrane (Figure 3E). The formation of apical tight junctions around BrdU-positive cells was indicated by the localization of zonula occludens 1 (ZO-1) (Figure 3F). The presence of proliferating AQP3-expressing cells indicates that collecting duct cells were injured and regenerated in this model of IRI.

Intrinsic renal cells are the major source of renal regeneration. The relative contribution of tubule-derived cells and BMC-derived cells to renal regeneration was analyzed in 6- to 8-week-old wild-type con-

Table 1

Renal cells are the main source of tubular regeneration

No. of tubular cells	No. of BrdU+ cells	No. of Y+ cells	% BrdU+ cells	% Y+ cells
1,051 ± 131	97 ± 19	6.7 ± 1.0	9 ± 1.1	1 ± 0.1

Y chromosome FISH was followed by immunostaining of BrdU. Total BrdU+– and Y chromosome–positive (Y+) nuclei in the tubules were counted in 10 randomly selected fields in the outer stripe of outer medulla. The percent of Y+ cells was adjusted for the 64% sensitivity of Y chromosome FISH. The values represent mean ± SE; n = 4.

AQP3, which indicated that they were principal cells (Figure 4F). In addition, the labeling of the basolateral membrane by AQP3 clearly defines the intratubular localization of BMC-derived cells. Taken together, these results indicate that BMCs can differentiate into tubular epithelial cells that express tubular structural proteins and water channels. When BMCs isolated from male *crekSp;Z/EG* mice were transplanted into wild-type female mice with renal IRI, no native EGFP fluorescence or EGFP expression by immunostaining was detected, although Y chromosome–positive cells were present in renal tubules (Figure 4, G and H). This result indicates that the EGFP-positive cells that were observed in the kidney were not derived from BMCs.

BMCs make a minor contribution to renal repair. Renal IRI causes decreased glomerular filtration rate and elevated blood urea nitrogen (BUN) levels. Following IRI, glomerular filtration rate (GFR) returns to near baseline within 1 week (29). We measured BUN levels in sham-operated mice without BMC injection and in mice with left renal IRI with or without BMC injection. BMCs were harvested from male B6-Ly5.2/Cr mice that carry CD45.1 and were injected into recipient female C57BL/6NCr mice that carry CD45.2. The right kidney was removed to eliminate its contribution to GFR. BUN levels were 20 ± 2 mg/dl in sham-operated mice 1 day after surgery. In contrast, mice that underwent renal IRI without BMC injection had elevated BUN levels of 87 ± 8 mg/dl. BMC injection did not reduce BUN levels (91 ± 12 mg/dl) in mice with renal IRI (Figure 4I). There was no statistically significant difference in BUN levels in mice with or without BMC injection between 1 and 7 days after injury (n = 5–13 at each time point; total 84 mice). The absence of improved renal function was not due to the failure of BMC transplantation. Flow cytometry analysis at 28 days showed that 38% of the peripheral nucleated cells carried the CD45.1 donor cell marker, which indicated successful engraftment of BMCs.

The absence of a renal protective effect suggested that transplanted BMCs made only a limited contribution to kidney regeneration in the first week after injury. We found that Y chromosome–positive cells began to appear in the interstitium and glomeruli as early as 2 days after injury. However, the earliest time point at which Y chromosome–positive cells could be detected in the tubules was 5 days. At 7 days, only 1 or 2 tubular cells/section were Y chromosome positive, and no more than 8 total Y chromosome–positive cells/kidney section could be detected.

BMCs can form multiple types of glomerular cells. In addition to forming epithelial cells, transplanted BMCs also differentiated into glomerular and interstitial cells. In the kidney, the number of Y chromosome–positive cells increased with time after injury. We counted the total number of Y chromosome–positive cells in the kidney as

well as Y chromosome–positive cells in the tubules, glomeruli, and interstitium at 28 days after IRI (n = 4). Ten fields of the cortex and medulla were randomly selected for counting. The results are summarized in Table 2. An average of 52 Y chromosome–positive cells per 1,011 kidney cells were detected. This implies that 8% of the total number of kidney cells were donor-derived, after correction was made for the 64% sensitivity of Y chromosome FISH. Among these cells, 8.4% were tubular epithelial cells, 10.6% were glomerular cells, and 81% were interstitial cells (Figure 5).
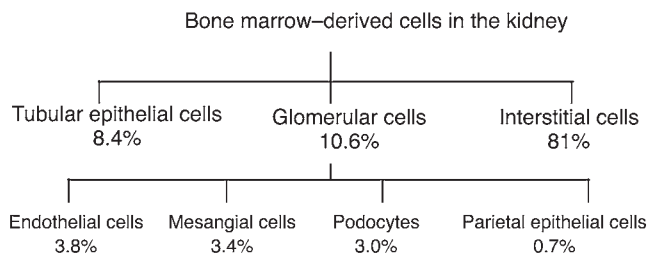
The formation of glomerular cells from BMCs was examined in greater detail. Of 436 glomeruli counted, 180 (41%) contained 1–4 Y chromosome–positive cells/glomerulus (Figure 6A). Of 316 glomeruli counted, only 1 CD45-positive cell was detected (data not shown). Since common leukocyte antigen CD45 is only expressed on the cell surface of hematopoietic cells, the rarity of CD45-positive cells indicated that the majority of hematopoietic cells in the glomeruli had differentiated into non-hematopoietic cells. Alternatively, mesenchymal stem cells in the BMCs could have contributed to glomerular cell formation. To identify endothelial cells, we stained the kidney sections with *Lycopersicon esculentum* lectin (LEL) (30). Donor-derived cells were CD45-negative and LEL-positive, which suggested endothelial formation from transplanted BMCs (Figure 6B). Some donor-derived cells in the glomeruli expressed vimentin and did not express Wt1, which suggested that they were mesangial cells (Figure 6C). Donor-derived podocytes expressing Wt1 (31) were also detected (Figure 6D). Among all donor-derived cells in the glomeruli, 35% were endothelial cells, 31% were mesangial cells, 27% were podocytes, and 7% were parietal epithelial cells (n = 4). Since a total of 10.6% of bone marrow–derived cells in the kidney formed glomerular cells, these values indicate that 3.8% of the BMCs formed endothelial cells, 3.4% formed mesangial cells, 3.0% formed podocytes, and 0.7% formed parietal epithelial cells (Figure 5).

Most bone marrow–derived cells in the kidney do not continue hematopoiesis and may contribute to interstitial fibrosis. Because long-term hematopoietic stem cells can adopt a traditional hematopoietic cell fate when injected into the ischemic myocardium (32), we studied the developmental potential of BMCs in the kidney. Examination of 4 serial sections of 5 different kidneys showed that none of the BrdU-positive cells in the tubules expressed CD45, and no Y chromosome and CD45 double-positive cells were detected in the tubules, which indicated that a switch to a non-hematopoietic lineage had occurred in the renal tubules. However, in the interstitium, an average of 11% of the cells were Y chromosome and CD45 double-positive at 28 days. Figure 7A

Table 2

Y chromosome–positive cells in the kidneys at 28 days after IRI

	No. of nuclei counted	% Y+ nuclei/total nuclei
Total nuclei	1,011 ± 155	N/A
Y+ nuclei	52 ± 4	8.03 ± 0.57
Y+ tubular cells	5.1 ± 0.9	0.78 ± 0.14
Y+ glomerular cells	9.0 ± 1.2	0.88 ± 0.17
Y+ interstitial cells	41.0 ± 3.0	6.42 ± 0.46

Y chromosome FISH was performed, and the numbers of Y+ nuclei in the tubules, glomeruli and interstitium were counted. The percent of Y+ cells in the kidney was adjusted for the 64% sensitivity of Y chromosome FISH. The values represent mean ± SE; n = 4.

Bone marrow–derived cells in the kidney

Tubular epithelial cells
8.4%

Glomerular cells
10.6%

Interstitial cells
81%

Endothelial cells
3.8%

Mesangial cells
3.4%

Podocytes
3.0%

Parietal epithelial cells
0.7%

Figure 5
Formation of renal cells from bone marrow–derived cells. The total of 8% of bone marrow–derived cells in the kidney consisted of tubular epithelial cell, glomerular cells, and interstitial cells. The relative percentages of different cell types are shown.

shows the presence of multiple Y chromosome–positive cells in the interstitium, and the inset depicts a Y chromosome and CD45 double-positive cell in the interstitium. A total of 2% and 7% CD45 positive cells incorporated BrdU at 14 and 28 days, respectively. These results suggest that most of the BMCs in the kidney do not undergo continuous hematopoiesis.

The increase in donor-derived cells in the kidney was mostly observed in the interstitium. At 28 days, 29% of all interstitial cells were Y chromosome positive. Donor cells expressing α-SMA, a marker for myofibroblasts, were detected (Figure 7B). Trichrome staining showed collagenous interstitial lesions and fibrosis (Figure 7C). In contrast, the kidney that had recovered from IRI but did not receive BMC injection showed minimal collagen accumulation in the interstitium (Figure 7D). These results suggest that transplanted BMCs may be involved in renal interstitial fibrosis.

Discussion

We generated *cre^{ksp};Z/EG* mice that expressed EGFP specifically and permanently in renal tubular epithelial cells and subjected them to unilateral renal ischemic injury. The incorporation of BrdU and expression of vimentin in EGFP-expressing cells in the ischemic kidney, but not in the contralateral nonischemic kidney, provide direct evidence that intrarenal cells can regenerate to repair injured tubules. Because vimentin is not normally expressed in mature tubular epithelial cells and EGFP is only expressed in the mature epithelial cells and their progeny, coexpression of vimentin and EGFP indicates dedifferentiation of surviving tubular epithelial cells. Consistent with these findings, expression of Pax2 was upregulated in regenerating proximal tubular cells, and expression of the cyclin-dependent kinase inhibitor p21 was downregulated. Tubular regeneration via this mechanism was observed in the proximal tubule, a segment of the nephron that is particularly susceptible to ischemic injury, as well as in renal collecting ducts, which were not previously known to be a major site of ischemic injury and regeneration.

We estimated the quantitative contribution of intrarenal cells and extrarenal cells to tubular regeneration by infusion of BMCs to the mice with renal IRI. Previous studies have shown that bone marrow contains hematopoietic stem cells that can be incorporated into renal tubules after ischemic injury, but the magnitude of tubular regeneration from this source was not known. Following transplantation of BMCs from male donors into female recipients with IRI, 11% of the BrdU-positive tubular cells were donor-derived, whereas the majority of the proliferating cells, 89%, were derived from the

host. These results confirm that extrarenal bone marrow–derived cells can be incorporated into renal tubules after ischemic injury, but intrarenal cells are the major source of tubular regeneration.

In adult ischemic kidney, intrarenal cells consist of surviving tubular epithelial cells and renal stem cells. It has been hypothesized that the kidney contains residual metanephric stem cells that can differentiate into epithelial cells following tubular injury (33). Moreover, renal stem cells have been identified in the papilla of postnatal kidneys by BrdU labeling of slow-cycling cells (12). These stem cells would not express EGFP, which is only expressed in mature renal epithelial cells. However, once the progeny of renal stem cells differentiate into tubular epithelial cells, EGFP may be expressed. The unavailability of renal stem cell markers limits the tracing and quantification of stem cell progeny in postischemic kidney. In the present study, the EGFP-positive cells in the tubules were not derived from BMCs of *cre^{ksp};Z/EG* mice. This conclusion is supported by the observation that when we transplanted BMCs from male *cre^{ksp};Z/EG* mice into female wild-type mice with renal IRI, no EGFP-expressing cells were detected in the renal tubules. Although the mosaic expression of EGFP precluded a precise determination of the relative contribution of tubular cells and renal stem cells to renal regeneration, the observation that the regenerating kidney contained more EGFP-positive proximal tubular cells than the contralateral control kidney is consistent with the hypothesis that the majority of regenerating tubular cells originated from mature tubular cells and argues against a major contribution of BMCs to tubular repair.

The mechanism of tubular epithelial cell dedifferentiation is not understood. It is believed that tubular regeneration recapitulates tubulogenesis during fetal kidney development. The permanent
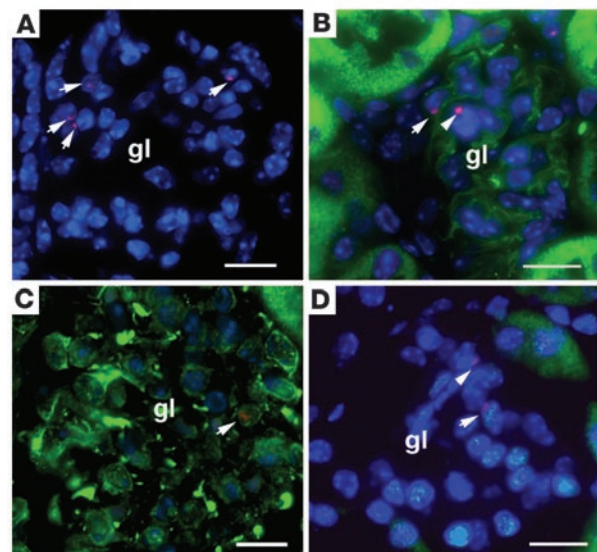
Figure 6
Formation of glomerular cells from BMCs. Y chromosome FISH (red) was followed by immunostaining for markers of glomerular cells. (**A**) Arrows indicate Y$^+$ CD45$^-$ cells in the glomerulus. (**B**) The arrow indicates a Y$^+$ LEL$^+$ endothelial cell. LEL is labeled green. The arrowhead indicates a Y$^+$ LEL$^-$ cell. (**C**) The arrow indicates a Y$^+$ vimentin$^+$Wt1$^-$ mesangial cell. Wt1 is labeled blue in the nuclei. (**D**) The arrow indicates Y$^+$ Wt1$^+$ podocyte. Wt1 is labeled green in the nuclei. The arrowhead indicates a Y$^+$ Wt1$^-$ cell. The nuclei were counterstained with DAPI (**A**, **B**, and **D**), and images were merged. Scale bars: 20 μm.
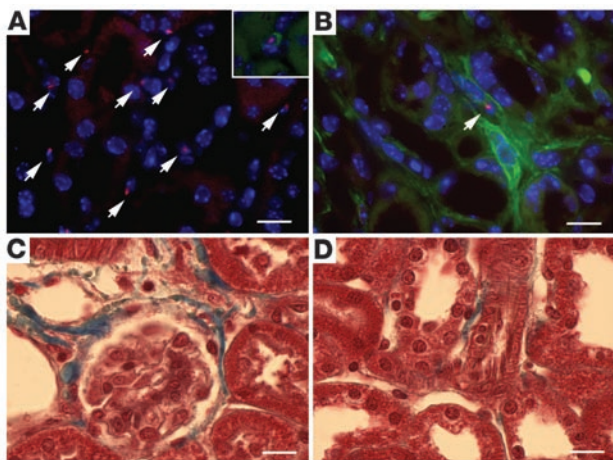
Figure 7
Formation of interstitial cells from BMCs. (**A**) Y chromosome FISH shows abundant Y+ cells (red, arrows) in the interstitium. The inset shows a Y+ CD45+ cell detected in the interstitium. (**B**) The arrow indicates a Y+ α-SMA+ myofibroblast. (**C**) Trichrome stain shows prominent collagenous deposit and fibrosis in the kidney of mouse with IRI that received BMC injection. (**D**) Trichrome staining shows minimal collagenous formation in the kidney of mouse with IRI that did not receive BMC injection. The nuclei were counterstained with DAPI (**A** and **B**), and images were merged. Scale bars: 20 μm.

kidney, the metanephros, develops from reciprocal interactions between the ureteric bud, which gives rise to the renal collecting system, and the metanephric mesenchyme, which forms the nephrons. Upon induction by the ureteric bud, metanephric mesenchymal cells undergo a mesenchymal-epithelial transition and differentiate into tubular epithelial cells. Expression of Pax2 begins in condensed metanephric mesenchyme and continues in comma- and S-shaped bodies, which are the anlagen of the nephron, including proximal tubules (34, 35). As tubulogenesis proceeds, Pax2 is downregulated, and mature proximal tubules do not express Pax2. The reexpression of Pax2 in proximal tubular cells following injury suggests a reversion to an immature precursor cell phenotype. In cells that express Pax2, the cyclin-dependent kinase inhibitor p21 is downregulated, which suggests cell cycle reentry in regenerating cells. At the same time, the intermediate filament, vimentin, is expressed in the epithelial cells. Vimentin is a marker for mesenchymal cells and is not normally expressed in tubular epithelial cells (36). Reexpression of vimentin in EGFP-expressing tubular epithelial cells suggests reversion of epithelial cells to a mesenchymal cell–like phenotype. Twenty-eight days after injury, as regeneration is completed, the tubular cells regain mature epithelial cell polarity and intercellular junctions, and vimentin is no longer expressed.

Unlike in organisms such as urodele amphibians that have the ability to regenerate a wide variety of tissues via dedifferentiation mechanisms, regeneration in mammals is limited. However, regeneration from differentiated cells has been described in mice. Recently, Dor et al. showed that preexisting pancreatic β cells formed new β cells during adult life and after pancreatectomy (10). Terminally differentiated mouse myotubes can dedifferentiate and reenter the cell cycle when treated with an extract from regenerating newt limb tissue (37). Moreover, myotube-derived mononucleated cells can be induced to redifferentiate into cells expressing chondrogenic, adipogenic, myogenic, and osteogenic

markers when the homeobox-containing transcriptional repressor *msx1* is expressed ectopically in mouse myotubes (38). These findings suggest that terminally differentiated mammalian cells have the ability to become progenitors with appropriate stimuli. In *Drosophila,* germline stem cells can be generated by spermatogonial dedifferentiation (39). Our results show that dedifferentiated epithelial cells reenter the cell cycle to proliferate and regenerate renal tubules. At present, the full developmental potential of these cells is not clear; nor is it clear whether they contribute to renal turnover under normal conditions. However, the absence of BrdU incorporation in EGFP-expressing cells in the uninjured kidney suggests that mature epithelial cells may not participate significantly in normal renal turnover.

Renal function usually recovers in 1–2 weeks after IRI. Few bone marrow–derived cells were detected in kidney tubules at 7 days after injury, which suggests that recovery largely depends on tubular regeneration from endogenous kidney cells. Consistent with this hypothesis, administration of BMCs did not improve renal function in mice with ischemic injury. These results are in contrast to those from a study by Kale et al., who reported improvement of renal function with hematopoietic stem cell transplantation in mice with renal IRI (17). Kale et al. used sorted hematopoietic stem cells and performed bilateral IRI, whereas whole BMCs were used and unilateral IRI with contralateral nephrectomy was performed in the present study. It is possible that in the study performed by Kale et al., more hematopoietic stem cells and their progeny entered the kidneys to augment functional recovery.

Previously we showed that sorted Lin−Sca-1+ckit+ hematopoietic stem cells contributed to renal tubular cell formation following IRI. Mesenchymal stem cells that reside in the bone marrow also have plasticity in forming multiple types of cells of mesenchymal and non-mesenchymal lineages (40, 41). Formation of renal tubular cells from mouse bone marrow–derived mesenchymal cells has been reported (23). The current study aimed to comprehensively analyze the types and percentages of renal cells that originated from unfractionated BMCs in postischemic kidneys. No CD45-positive cells were detected in the renal tubules. Since CD45 is only present in the hematopoietic cells and not in the mesenchymal cell, the absence of CD45-positive cells in the renal tubules could suggest conversion of hematopoietic cells to renal cells and/or formation of renal tubular cells from mesenchymal stem cells.

Formation of glomerular cells and endothelial cells from BMCs has been reported in several studies. Poulsom et al. observed donor BMC-derived podocytes in mouse kidney that was subjected to total body irradiation but no other injury (19), which suggested that BMCs have a role in normal glomerular turnover. In rats with chimeric bone marrow, donor BMC-derived mesangial cells and endothelial cells were detected (20). When glomerular injury was induced with anti–Thy-1.1 antibody, the number of donor BMC-derived endothelial cells increased 4-fold at 7 days and the number of mesangial cells increased 7-fold at 28 days after injury. We confirmed these findings by showing the presence of BMC-derived podocytes, endothelial cells, mesangial cells, and parietal epithelial cells in glomeruli in the kidney that had recovered from ischemic injury. In addition, the contribution of BMCs to different cell types was quantified. Most BMCs differentiated into renal interstitial cells, while a small percentage of them differentiated into glomerular cells, endothelial cells, and tubular epithelial cells.

The large number of BMC-derived interstitial cells, especially myofibroblasts, suggests the involvement of BMCs in fibrosis.

This is in agreement with the report by Iwano et al. that BMCs can differentiate into renal interstitial fibroblast (22). Renal IRI is accompanied by inflammatory cell infiltration, and the inflammation subsides after 10 days (42). Hematopoietic stem cell mobilization–associated granulocytosis can worsen acute renal failure in mice (43). The long-term consequence of allograft bone marrow transplantation in mice with IRI is not clear and may warrant further investigation. Our study calls for caution in premature clinical use of BMCs in the treatment of renal failure.

Methods

Renal IRI, bone marrow transplantation, and BUN level measurement. Six- to 8-week-old female C57BL/6NCr or *cre^{ksp};Z/EG* mice were irradiated with 9.0 Gy of γ-irradiation in 2 divided doses, 2 hours apart, on the day of surgery. Mice were anesthetized with isoflurane, and the left renal pedicles were clamped with vascular clamps for 45 minutes, which was followed by clamp release to allow reperfusion. Right nephrectomy was performed in some mice. Sham-operated mice underwent the same procedures except for clamping of the renal vessels. BMCs were isolated from the femur and tibia of male C57BL/6 or B6-Ly5.2/Cr mice by flushing with Iscove's minimal essential medium (IMEM). Mice were injected with 0.2 ml IMEM with or without 1×10^6 BMCs via tail veins at 2 hours after surgery. Mice were kept in a specific pathogen–free facility and were given drinking water containing enrofoxacin (0.15 mg/ml) and amoxicillin (1 mg/ml) for 2 weeks to prevent infection. Some mice were given 50 μg/g BrdU or saline at 0.1 ml i.p. for 14 days. After whole-body perfusion via the left ventricle with 30 ml PBS to remove the blood, the kidneys were harvested and processed for cryosections or paraffin sections as described previously (16). Blood was obtained via retro-orbital puncture, and BUN levels were measured using a Reflotron analyzer (Roche Diagnostic Corp.). All experiments were performed with the approval of the Institutional Animal Care and Research Advisory Committee, University of Texas Southwestern Medical Center at Dallas, Dallas, Texas, USA.

Y chromosome FISH analysis. The mouse Y chromosome painting probe was generated by degenerate oligonucleotide–primed PCR using a DNA template kindly provided by Diane Krause (Yale University, New Haven, Connecticut, USA) and labeled with digoxigenin by nick translation, as described previously (44). Y chromosome FISH analysis was performed on formalin-fixed and paraffin-embedded kidney sections (4 μm in thickness) using methods described previously (27). Cy-3–conjugated mouse anti-digoxigenin (Jackson ImmunoResearch Laboratories) was used to visualize Y chromosome signals. Kidneys from normal male and female mice that did not receive male BMC injection were used to test the sensitivity and specificity of Y chromosome FISH analysis, respectively. The sensitivity was determined by calculating the number of Y chromosome–positive nuclei divided by total nuclei [(Y⁺ nuclei ÷ total nuclei) × 100%].

Immunohistochemistry. Immunostaining was performed on paraffin sections (4 μm in thickness) as described previously (16). Briefly, the kidney sections were incubated at 4°C overnight with antibodies to GFP (1:00;

Invitrogen Corp.), BrdU (1:2.5; BD), Pax2 (1:50; Zymed Laboratories Inc.), vimentin (1:100; Chemicon International), p21 (1:200; Upstate), PCNA (1:00; Santa Cruz Biotechnology Inc.), pan-cytokeratin (1:500; Dako-Cytomation), AQP3 (1:400; Chemicon International), CD45 (1:50; CALTAG Laboratories), Wt1 (1:50; Santa Cruz Biotechnology Inc.), α-SMA (1:400; Sigma-Aldrich), ZO-1 (1:100, Upstate), THP (1:100; John Hoyer, Children's Hospital of Philadelphia, Philadelphia, Pennsylvania, USA) (45), TSC (1:00; Mark Knepper, NIH, Bethesda, Maryland, USA.) (46). After washing, the kidney sections were incubated with secondary antibodies for 1 hour at room temperature. Secondary antibodies included Alexa Fluor 488–conjugated goat anti-rabbit or goat anti-mouse IgG, Alexa Fluor 594–conjugated goat anti-rabbit IgG, and Alexa Fluor 350–conjugatedgoat anti-mouse IgG (1:400; Invitrogen Corp.). Some kidney sections were incubated with biotinylated anti-rat or anti-goat IgG followed by avidin-fluorescein (1:400; Vector Laboratories). Lectin staining was performed by incubation at room temperature for 2 hours with FITC-labeled LTA (1:50), DBA(1:40), or TEL (1:50) obtained from Vector Laboratories. The nuclei were counterstained with DAPI prior to visualization and photography under epifluorescence illumination using a Zeiss Axioplan microscope. Images were merged and analyzed using OpenLab software version 3.1.7.

Flow cytometry analysis of CD45.1 cells. Peripheral blood was collected via puncture of the retro-orbital vein. Red blood cells were lysed with 0.84% NH_4Cl. The nucleated blood cells were incubated with FITC-coupled anti-CD45.1 antibody (1:1,000; BD Biosciences — Pharmingen) and analyzed with flow cytometry (FACScan; BD).

Quantification and statistics. For quantification of immunostaining and Y chromosome FISH analysis, 10 fields (×630) from cortex and 10 fields (×630) from medulla were randomly selected for counting. Each immunostaining and Y chromosome FISH analysis was duplicated, and the values for quantification were averaged. The number of animals used is indicated for each individual experiment. Data are represented as mean ± SE. Student's *t* test was performed using 2-tailed distribution. $P < 0.05$ was considered to be statistically significant.

Address correspondence to: Fangming Lin, Department of Pediatrics, University of Texas Southwestern Medical Center at Dallas, Dallas, Texas 75390-9063, USA. Phone: (214) 648-3438; Fax: (214) 648-2034; E-mail: Fangming.lin@utsouthwestern.edu.

1. Bonventre, J.V. 1993. Mechanisms of ischemic acute renal failure. *Kidney Int.* **43**:1160–1178.
2. Savill, J. 1994. Apoptosis and the kidney. *J. Am. Soc. Nephrol.* **5**:12–21.
3. Witzgall, R., Brown, D., Schwarz, C., and Bonventre, J.V. 1994. Localization of proliferating cell nuclear antigen, vimentin, c-Fos, and clusterin in the postischemic kidney. Evidence for a heterogenous genetic response among nephron segments, and a large pool of mitotically active and dedifferentiated cells. *J. Clin. Invest.* **93**:2175–2188.
4. Weissman, I.L. 2000. Stem cells: units of development, units of regeneration, and units in evolution [review]. *Cell.* **100**:157–168.
5. Metcalf, D. 1999. Stem cells, pre-progenitor cells and lineage-committed cells: are our dogmas correct [review]? *Ann. N. Y. Acad. Sci.* **872**:289–303; discussion 303–304.
6. Lie, D.C., Song, H., Colamarino, S.A., Ming, G.L., and Gage, F.H. 2004. Neurogenesis in the adult brain: new strategies for central nervous system diseases [review]. *Annu. Rev. Pharmacol. Toxicol.* **44**:399–421.
7. Brittan, M., and Wright, N.A. 2004. The gastrointestinal stem cell [review]. *Cell Prolif.* **37**:35–53.
8. Alison, M.R., et al. 2004. Hepatic stem cells: from inside and outside the liver [review]? *Cell Prolif.* **37**:1–21.
9. Odelberg, S.J. 2002. Inducing cellular dedifferentiation: a potential method for enhancing endogenous regeneration in mammals [review]. *Semin. Cell Dev. Biol.* **13**:335–343.
10. Dor, Y., Brown, J., Martinez, O.I., and Melton, D.A. 2004. Adult pancreatic beta-cells are formed by self-duplication rather than stem-cell differentiation. *Nature.* **429**:41–46.
11. Krause, D.S., et al. 2001. Multi-organ, multi-lineage engraftment by a single bone marrow-derived stem cell. *Cell.* **105**:369–377.

12. Oliver, J.A., Maarouf, O., Cheema, F.H., Martens, T.P., and Al-Awqati, Q. 2004. The renal papilla is a niche for adult kidney stem cells. *J. Clin. Invest.* **114**:795–804. doi:10.1172/JCI200420921.

13. Supavekin, S., et al. 2003. Differential gene expression following early renal ischemia/reperfusion. *Kidney Int.* **63**:1714–1724.

14. Imgrund, M., et al. 1999. Re-expression of the developmental gene Pax-2 during experimental acute tubular necrosis in mice 1. *Kidney Int.* **56**:1423–1431.

15. Megyesi, J., Andrade, L., Vieira, J.M., Jr., Safirstein, R.L., and Price, P.M. 2002. Coordination of the cell cycle is an important determinant of the syndrome of acute renal failure. *Am. J. Physiol. Renal Physiol.* **283**:F810–F816.

16. Lin, F., et al. 2003. Hematopoietic stem cells contribute to the regeneration of renal tubules after renal ischemia-reperfusion injury in mice. *J. Am. Soc. Nephrol.* **14**:1188–1199.

17. Kale, S., et al. 2003. Bone marrow stem cells contribute to repair of the ischemically injured renal tubule. *J. Clin. Invest.* **112**:42–49. doi:10.1172/JCI200317856.

18. Gupta, S., Verfaillie, C., Chmielewski, D., Kim, Y., and Rosenberg, M.E. 2002. A role for extrarenal cells in the regeneration following acute renal failure. *Kidney Int.* **62**:1285–1290.

19. Poulsom, R., et al. 2001. Bone marrow contributes to renal parenchymal turnover and regeneration. *J. Pathol.* **195**:229–235.

20. Rookmaaker, M.B., et al. 2003. Bone-marrow-derived cells contribute to glomerular endothelial repair in experimental glomerulonephritis. *Am. J. Pathol.* **163**:553–562.

21. Ito, T., Suzuki, A., Imai, E., Okabe, M., and Hori, M. 2001. Bone marrow is a reservoir of repopulating mesangial cells during glomerular remodeling. *J. Am. Soc. Nephrol.* **12**:2625–2635.

22. Iwano, M., et al. 2002. Evidence that fibroblasts derive from epithelium during tissue fibrosis. *J. Clin. Invest.* **110**:341–350. doi:10.1172/JCI200215518.

23. Morigi, M., et al. 2004. Mesenchymal stem cells are renotropic, helping to repair the kidney and improve function in acute renal failure. *J. Am. Soc. Nephrol.* **15**:1794–1804.

24. Novak, A., Guo, C., Yang, W., Nagy, A., and Lobe, C.G. 2000. Z/EG, a double reporter mouse line that expresses enhanced green fluorescent protein upon Cre-mediated excision. *Genesis.* **28**:147–155.

25. Shao, X., Somlo, S., and Igarashi, P. 2002. Epithelial-specific Cre/lox recombination in the developing kidney and genitourinary tract. *J. Am. Soc. Nephrol.* **13**:1837–1846.

26. Shao, X., Johnson, J.E., Richardson, J.A., Hiesberger, T., and Igarashi, P. 2002. A minimal ksp-cadherin promoter linked to a green fluorescent protein reporter gene exhibits tissue-specific expression in the developing kidney and genitourinary tract. *J. Am. Soc. Nephrol.* **13**:1824–1836.

27. Trotman, W., Beckett, T., Goncz, K.K., Beatty, B.G., and Weiss, D.J. 2004. Dual Y chromosome painting and in situ cell-specific immunofluorescence staining in lung tissue: an improved method of identifying donor marrow cells in lung following bone marrow transplantation. *Histochem. Cell Biol.* **121**:73–79.

28. Venkatachalam, M.A., Bernard, D.B., Donohoe, J.F., and Levinsky, N.G. 1978. Ischemic damage and repair in the rat proximal tubule: differences among the S1, S2, and S3 segments. *Kidney Int.* **14**:31–49.

29. Humes, H.D., Cieslinski, D.A., Coimbra, T.M., Messana, J.M., and Galvao, C. 1989. Epidermal growth factor enhances renal tubule cell regeneration and repair and accelerates the recovery of renal function in postischemic acute renal failure. *J. Clin. Invest.* **84**:1757–1761.

30. Thurston, G., Baluk, P., Hirata, A., and McDonald, D.M. 1996. Permeability-related changes revealed at endothelial cell borders in inflamed venules by lectin binding. *Am. J. Physiol.* **271**:H2547–H2562.

31. Charles, A.K., Mall, S., Watson, J., and Berry, P.J. 1997. Expression of the Wilms' tumour gene WT1 in the developing human and in paediatric renal tumours: an immunohistochemical study. *Mol. Pathol.* **50**:138–144.

32. Balsam, L.B., et al. 2004. Haematopoietic stem cells adopt mature haematopoietic fates in ischaemic myocardium. *Nature.* **428**:668–673.

33. Oliver, J.A., Barasch, J., Yang, J., Herzlinger, D., and Al-Awqati, Q. 2002. Metanephric mesenchyme contains embryonic renal stem cells. *Am. J. Physiol. Renal Physiol.* **283**:F799–F809.

34. Dressler, G.R., and Douglass, E.C. 1992. Pax-2 is a DNA-binding protein expressed in embryonic kidney and Wilms tumor. *Proc. Natl. Acad. Sci. U. S. A.* **89**:1179–1183.

35. Rothenpieler, U.W., and Dressler, G.R. 1993. Pax-2 is required for mesenchyme-to-epithelium conversion during kidney development. *Development.* **119**:711–720.

36. Holthofer, H., Miettinen, A., Lehto, V.P., Lehtonen, E., and Virtanen, I. 1984. Expression of vimentin and cytokeratin types of intermediate filament proteins in developing and adult human kidneys. *Lab. Invest.* **50**:552–559.

37. McGann, C.J., Odelberg, S.J., and Keating, M.T. 2001. Mammalian myotube dedifferentiation induced by newt regeneration extract. *Proc. Natl. Acad. Sci. U. S. A.* **98**:13699–13704.

38. Odelberg, S.J., Kollhoff, A., and Keating, M.T. 2000. Dedifferentiation of mammalian myotubes induced by msx1. *Cell.* **103**:1099–1109.

39. Brawley, C., and Matunis, E. 2004. Regeneration of male germline stem cells by spermatogonial dedifferentiation in vivo. *Science.* **304**:1331–1334.

40. Pittenger, M.F., et al. 1999. Multilineage potential of adult human mesenchymal stem cells. *Science.* **284**:143–147.

41. Roufosse, C.A., Direkze, N.C., Otto, W.R., and Wright, N.A. 2004. Circulating mesenchymal stem cells. *Int. J. Biochem. Cell Biol.* **36**:585–597.

42. Ysebaert, D.K., et al. 2000. Identification and kinetics of leukocytes after severe ischaemia/reperfusion renal injury. *Nephrol. Dial. Transplant.* **15**:1562–1574.

43. Togel, F., Isaac, J., and Westenfelder, C. 2004. Hematopoietic stem cell mobilization-associated granulocytosis severely worsens acute renal failure. *J. Am. Soc. Nephrol.* **15**:1261–1267.

44. Donnelly, D.S., Zelterman, D., Sharkis, S., and Krause, D.S. 1999. Functional activity of murine CD34+ and CD34- hematopoietic stem cell populations. *Exp. Hematol.* **27**:788–796.

45. Fasth, A., Hoyer, J.R., and Seiler, M.W. 1986. Renal tubular immune complex formation in mice immunized with Tamm-Horsfall protein. *Am. J. Pathol.* **125**:555–562.

46. Kim, G.H., et al. 1998. The thiazide-sensitive Na-Cl cotransporter is an aldosterone-induced protein. *Proc. Natl. Acad. Sci. U. S. A.* **95**:14552–14557.